Table of Content

Dynamics

A

Mentioned statement is true because on an astronomical scale flight in the atmosphere is close to surface of the earth that requires necessary assumption that the Earth can be considered flat. Although, rotation of the Earth makes calculations complicated, the Earth does not rotate that necessary assumption to make these calculations relatively simpler.

B

Longitudinal Stability

What express the motion in the pitch is called longitudinal stability. The horizontal stabilizer largely controls the longitudinal stability. The speed of the aircraft and the angle of attack affect the movement of the stabilizer. The quality that stabilizes an aircraft about its lateral axis is longitudinal stability

$$C_m = C_{m_0} + C_{m_\alpha}\alpha + C_{m_q}\frac{q\bar{c}}{2V} + C_{m_\delta}\delta_e + C_{m_M}M + C_{m_{F_T}} + F_T \quad (1)$$

$$C_m = \frac{M}{\bar{q}Sc} \quad (2)$$

$$C_{m_u} = {}^{U}\!/_{2}\frac{\partial C_m}{\partial u} \quad (3)$$

$$\frac{\rho SU\bar{c}}{I_y}(C_m + C_{m_u}) \quad (4)$$

Dimensional form of equation (3) $M_u = \frac{1}{I_y}\frac{\partial N}{\partial u} \quad 1/(met-s)$ (5)

$$C_{m_\propto} = \frac{\partial C_m}{\partial \alpha} \quad 1/rad \quad (6)$$

$$\frac{\rho SU\bar{c}}{2I_y}C_\alpha \quad 1/(met-s) \quad (7)$$

Dimensional form of equation (7) $M_w = \frac{1}{I_y}\frac{\partial M}{\partial w} \quad 1/(met-s)$ (8)

- For static stability and trim balance equation 2 should have positive value at 0° angle of attack.
- Sign of equation 3 can be change. The sign depends on Mach number and elastic properties.

- Equation 6 is preliminary design parameter. It defines the stick-fixed neutral point or static margin.

Static stability derivative can be derived from C_{m_α}.

$\frac{dC_m}{d\alpha}$ or C_{m_α} should be less than zero.

Directional Stability

What expresses the stability about the vertical axis of the aircraft is called directional stability. What controls the directional stability to a large extent is the vertical stabilizer. The primary flight control surface that moves the aircraft around the vertical or yaw axis is the rudder.

$$C_{n_\beta} = \frac{\partial C_n}{\partial \beta} > 0 \quad \text{and } C_n = 0 \; if \; \beta = 0$$

are the only expressions for derivation of directional stability.

Lateral Stability

Lateral stability is the stability around the longitudinal axis of the aircraft from nose to tail. When one wing is lowered than the wing on the other side of the airplane, positive lateral stability helps to compensate for lateral or "rolling effect".

$$C_{l_\beta} = \frac{\partial C_l}{\partial \beta} < 0 \; and \; C_l = 0 \; if \; \beta = 0$$

are the only expressions for derivation for lateral stability.

C

Phugoid motion is controlled by elevator. Thus, phugoid motion is performed on x axis. X axis component, and pitch angle and pitch rate terms from linearized longitudinal motion equations vary during short-period and phugoid motion.

D

It is a cambered airfoil. To analyse it, one of cambered airfoils of naca has been chosen. The chosen naca airfoil is NACA6409. It is analysed on xfoil with parameters which are mach number is 0.72 at angle of attack 4°. Pressure vectors on that airfoil are shown in the figure 1. According to figure 1, all pressure vectors are towards upward that is creating lift on this airfoil. Thus, pressure at point B is higher than pressure at point A. This occurs because the velocity at

point A is higher than the velocity at point B.

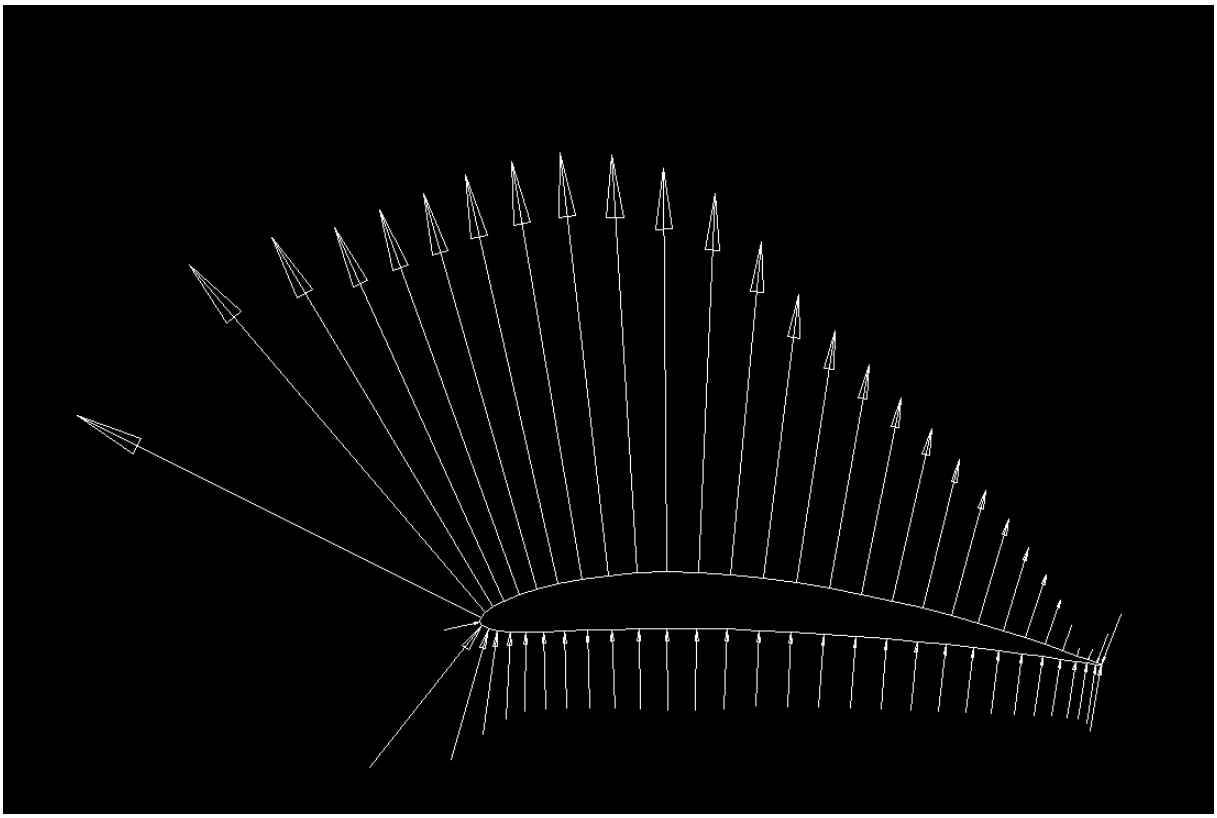

Figure 1 - Pressure Vector Analysis on NACA6409

E

a) It needs different angles of attack because they do not have horizontal and vertical stabiliser to do pitching and yawing motion. They can use these variations of angles of attack to perform pitching and yawing motions.
b) Flaps can be added to each rotating blades to change control surfaces of blades and this makes angle of attack different. These flaps can change control surfaces of every blades at the same time to different control surfaces. Thus, copter can perform different motions.

F

The most efficient is at the biggest ratio L/D that means higher the ratio of Cl/Cd higher efficiency. The highest Cl/Cd ratio is 12.5 at Cl = 0.5 from the figure 2a. thus, the most efficient angle of attack is 3.80 at Cl = 0.5 from the figure 2b.

G

a) In a short time-interval, it is less stable because the position of centre of mass will change. It will take time to stabilise it. After stabilised it, the helicopter will be more stable because centre of mass will be moved to the original position. Basically, in a short time-interval it is less stable. However, it is more stable in a long time-interval.

b)

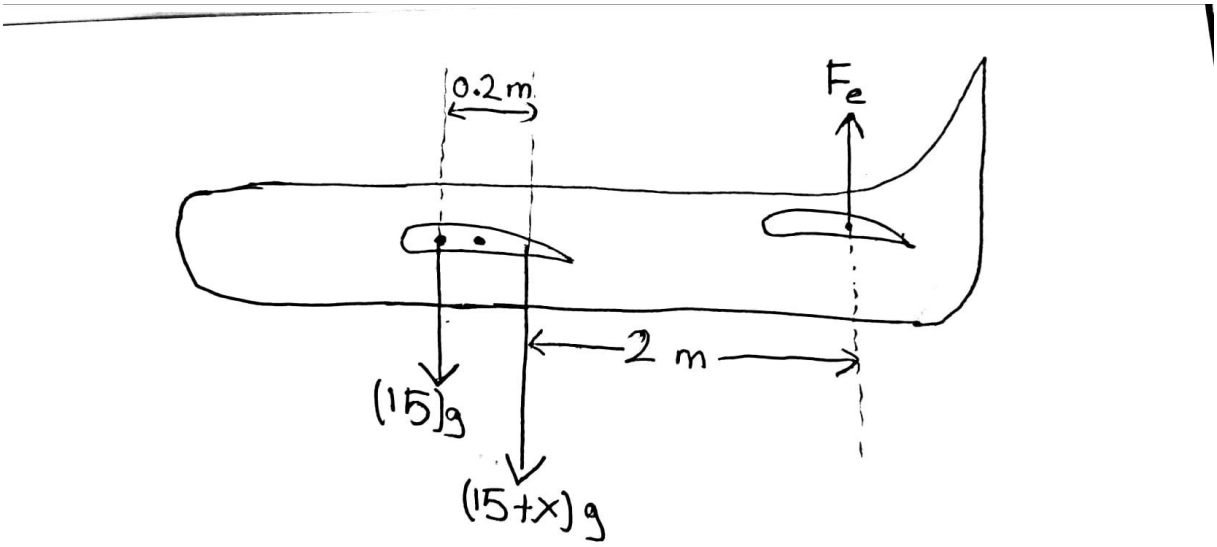

Figure 2 - Image of Calculations of Force of Elevator Deflection

To calculate the F_e, assuming aerodynamic centre of the wing is on the centre of gravity while it has payload is necessary because distance between old centre of gravity and aerodynamic centre, and mass of payload to calculate lift are not known. Thus,

$$\Sigma M_{x_{ac}} = (F_e)(2m) - (15kg)(g)(0.2m) = 0$$

$$(F_e)(2m) = (15kg)(g)(0.2m)$$

$$(F_e)(2m) = (15kg)\left(9.81\frac{m}{s^2}\right)(0.2m)$$

$$(F_e)(2m) = 29.43\ Nm$$

$$F_e = 14.715\ N$$

H

$$\begin{bmatrix} C_{X_u} - 2\mu_c D_c & C_{X_\alpha} & C_{Z_0} & 0 \\ C_{Z_u} & C_{Z_\alpha} + (C_{Z_{\dot{\alpha}}} - 2\mu_c) D_c & -C_{X_0} & 2\mu_c + C_{Z_q} \\ 0 & 0 & -D_c & 1 \\ C_{m_u} & C_{m_\alpha} + C_{m_{\dot{\alpha}}} D_c & 0 & C_{m_q} - 2\mu_c K_Y^2 D_c \end{bmatrix} \begin{bmatrix} u \\ \alpha \\ \theta \\ \frac{q\bar{c}}{V} \end{bmatrix} = \begin{bmatrix} -C_{X_{\delta_e}} \\ -C_{Z_{\delta_e}} \\ 0 \\ -C_{m_{\delta_e}} \end{bmatrix} \delta_e$$

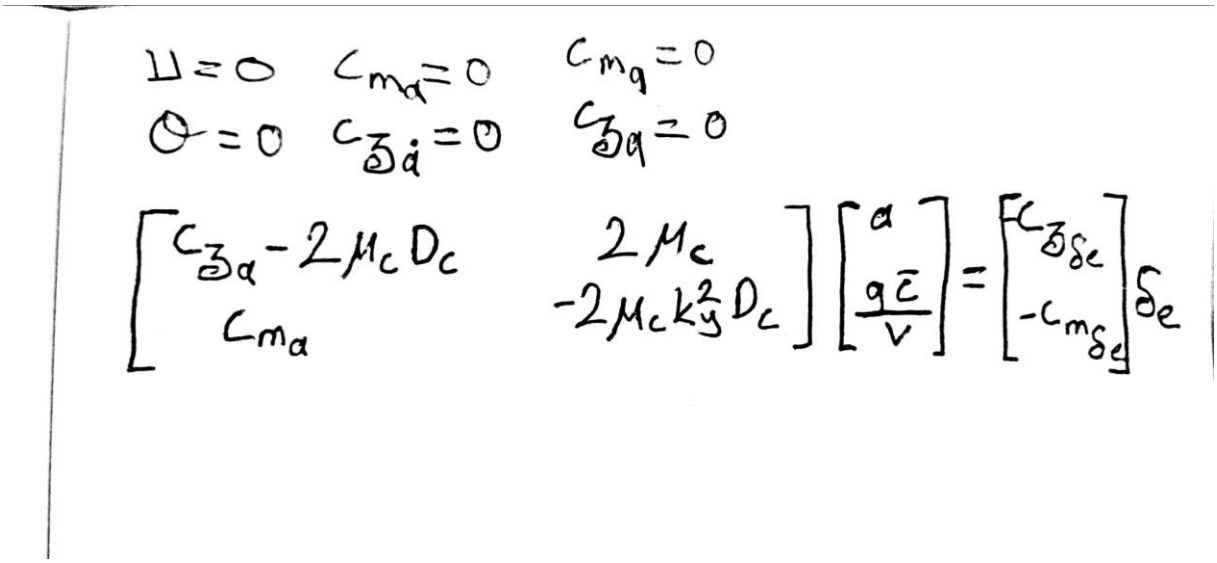

I

$$\lambda^2 + 2\zeta_s\omega_s\lambda + \omega_s^2 = A\lambda_c^2 + B\lambda_c + C$$

$$|A - \lambda I| = \begin{bmatrix} 0.5 - 410\lambda & 410 \\ -0.45 & -401.8\lambda \end{bmatrix}$$

D_c should be replaced with λ to determine the non-dimensional eigenvalues of the characteristic equation. Matrix in part G is used and the values on table 1 are used to find above matrix. Matlab code was written to find roots λ.

$$\lambda_{1,2} = 0.0006 \pm 0.0335i$$

Control

A

A and B matrices are given in the question and matlab codes (eigen command) are used to find eigenvalues of the uncontrolled plant. The system is stable because the eigenvalues are on the left half of the z-plane.

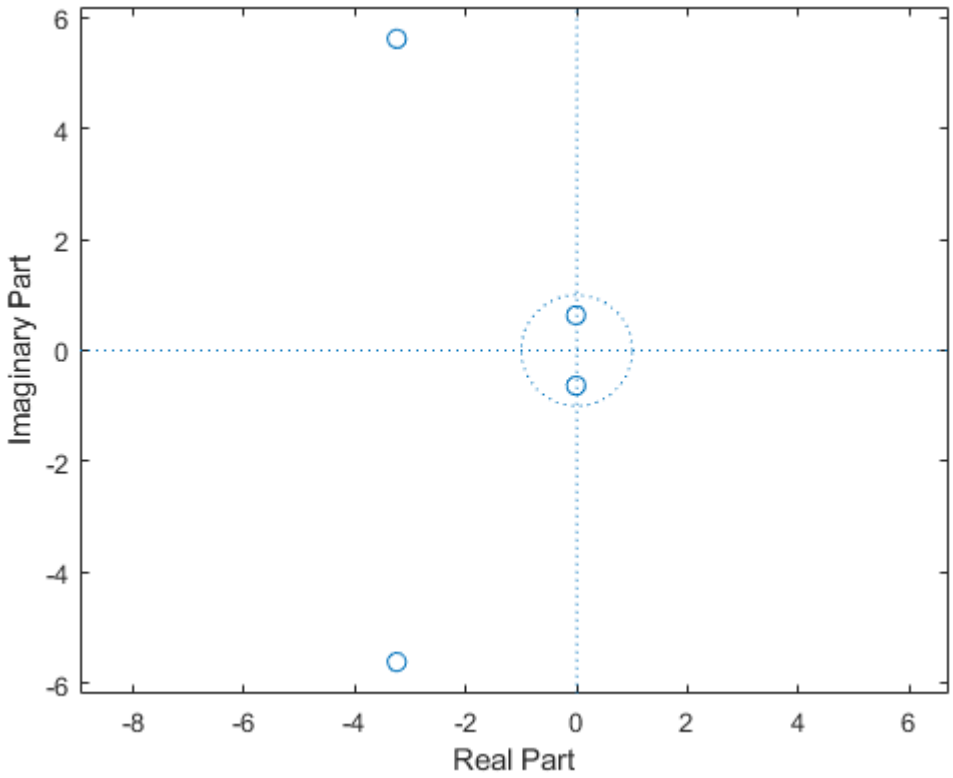

Figure 3 - Z-Plane for eigenvalues

B

C matrix is chosen as [0 0 0 1] for pitch angle because pitch angle is related to the last term of the C matrix from state space equation. C matrix is chosen as [0 0 1 0] for pitch rate because pitch rate is related to third term of the C matrix from state space equation. Lastly, D matrix is chosen as zero because there are no velocity terms neither on pitch angle nor on pitch rate. Using ss2tf command, numerators and denominators of transfer functions of both pitch angle and pitch rate are found. After that, transfer function of both pitch angle and pitch rate are found by using these numerators, denominators, and tf command. According to found eigenvalues of system the pole-zero maps are expected.

$$sys1 = \frac{-28.91s^2 - 89.96s - 15.56}{s^4\ 6.516\ s^3\ +\ 42.66\ s^2\ +\ 3.687\ s\ +\ 16.92}$$

Is the continuous-time transfer function for pitch angle

$K = -0.9195$ is low-frequency gain of the system.

$$sys2 = \frac{-28.91\ s^3\ -\ 89.96\ s^2\ -\ 15.56\ s\ -\ 8.768e-16}{s^4\ +\ 6.516\ s^3\ +\ 42.66\ s^2\ +\ 3.687\ s\ +\ 16.92}$$

Is the continuous-time transfer function for pitch rate

$L = -5.1831x10^{-17}$ is low-frequency gain of the system.

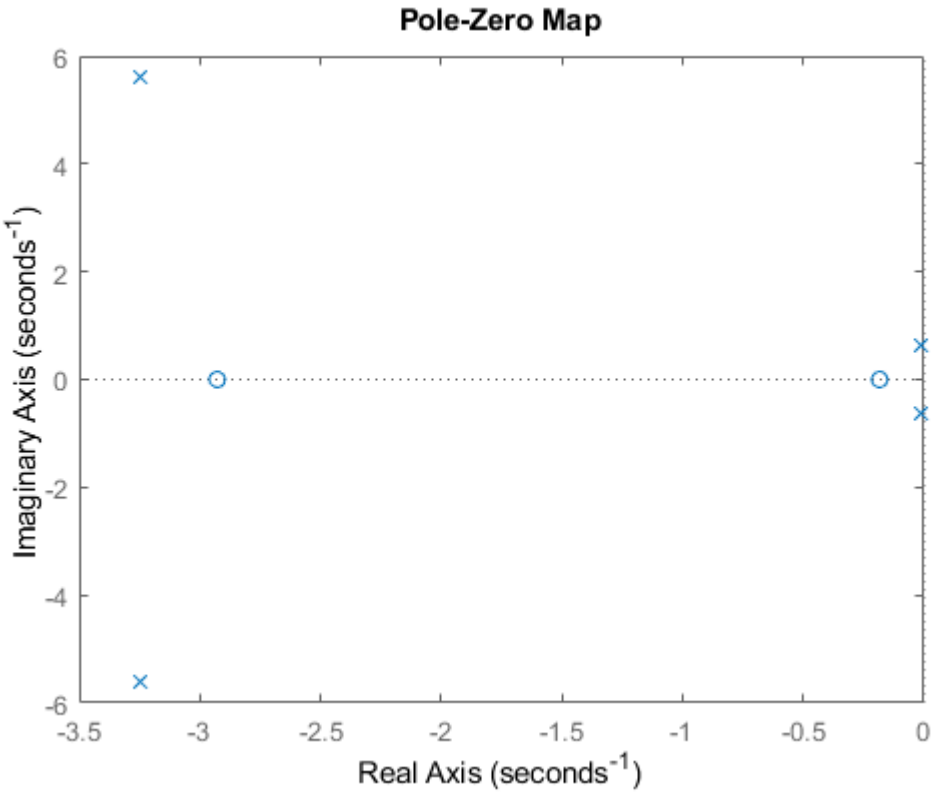

Figure 4- Pole-Zero Map for Pitch Angle

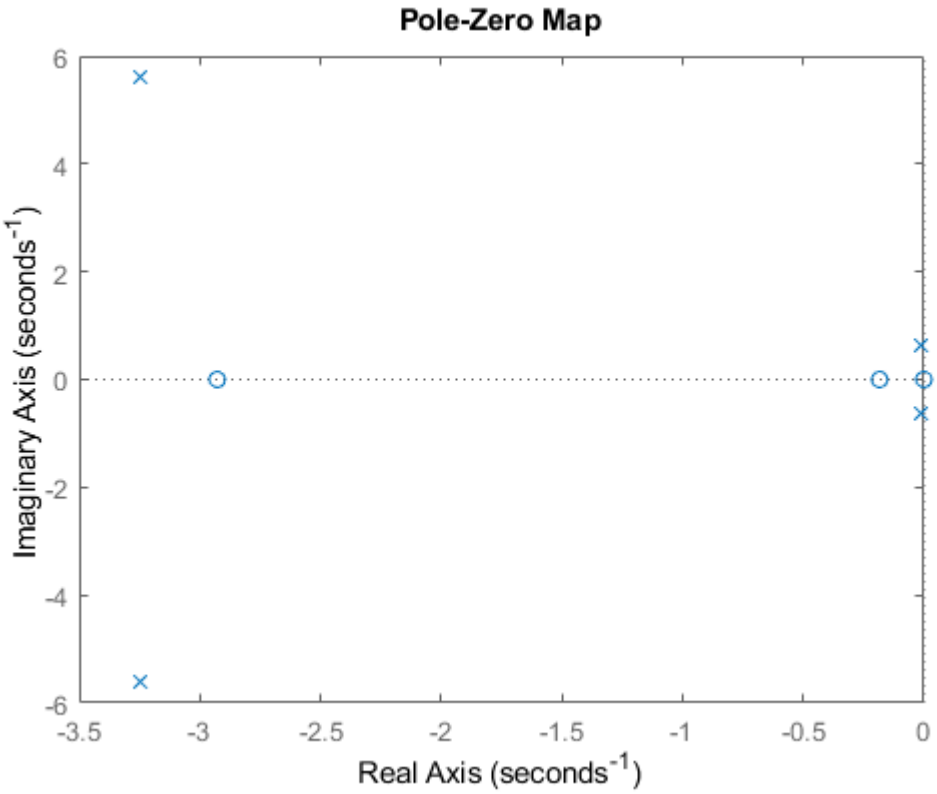

Figure 5 - Pole-Zero Map for Pitch Rate

C

Bode diagrams and Nyquist diagrams of the uncontrolled plant for pitch angle and pitch rate are found by using margin and Nyquist commands respectively. According to Nyquist plots, the distance between centre of each Nyquist plot on pitch angle is quite low and the distance between centre of each Nyquist plot on pitch rate is relatively high. Thus, it can be said that pitch angle transfer function is robust, but pitch rate transfer function is not robust.

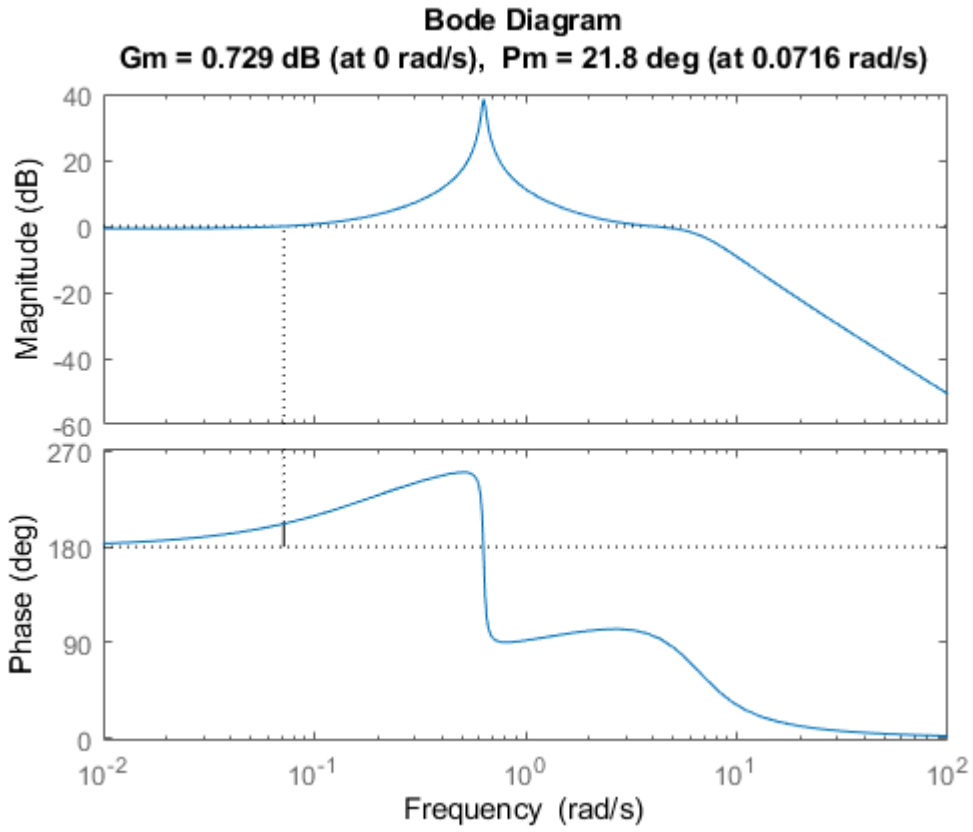

Figure 6 - Bode Diagram for Transfer Function of Pitch Angle

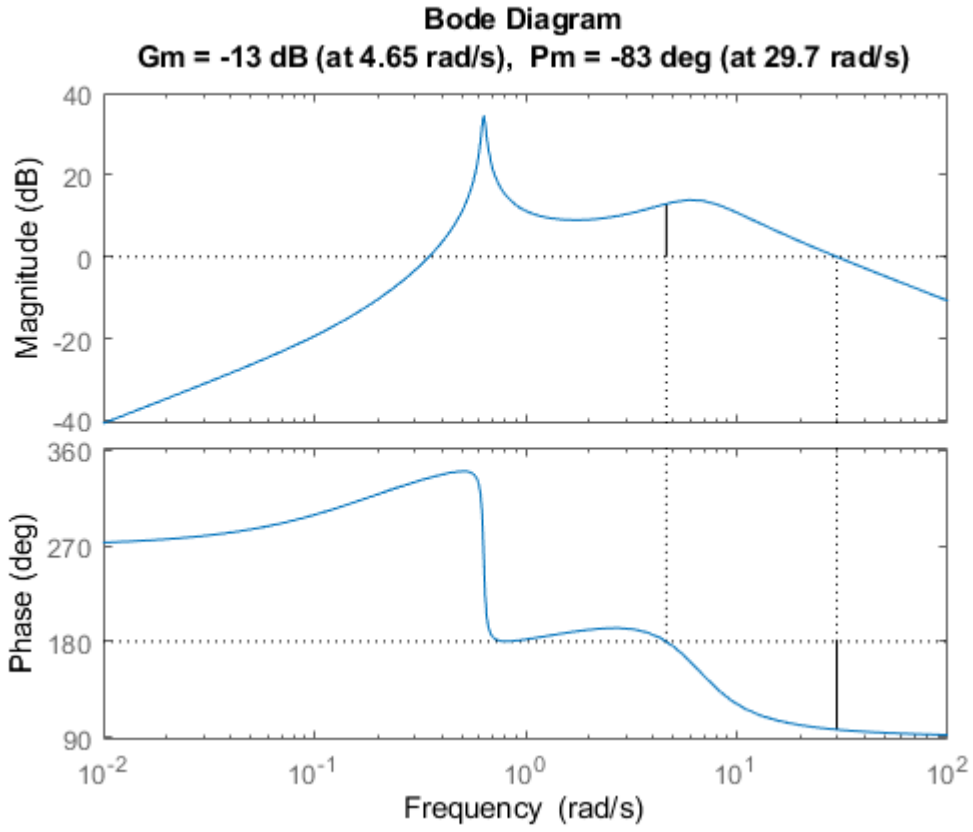

Figure 7 - Bode Diagram for Transfer Function of Pitch Rate

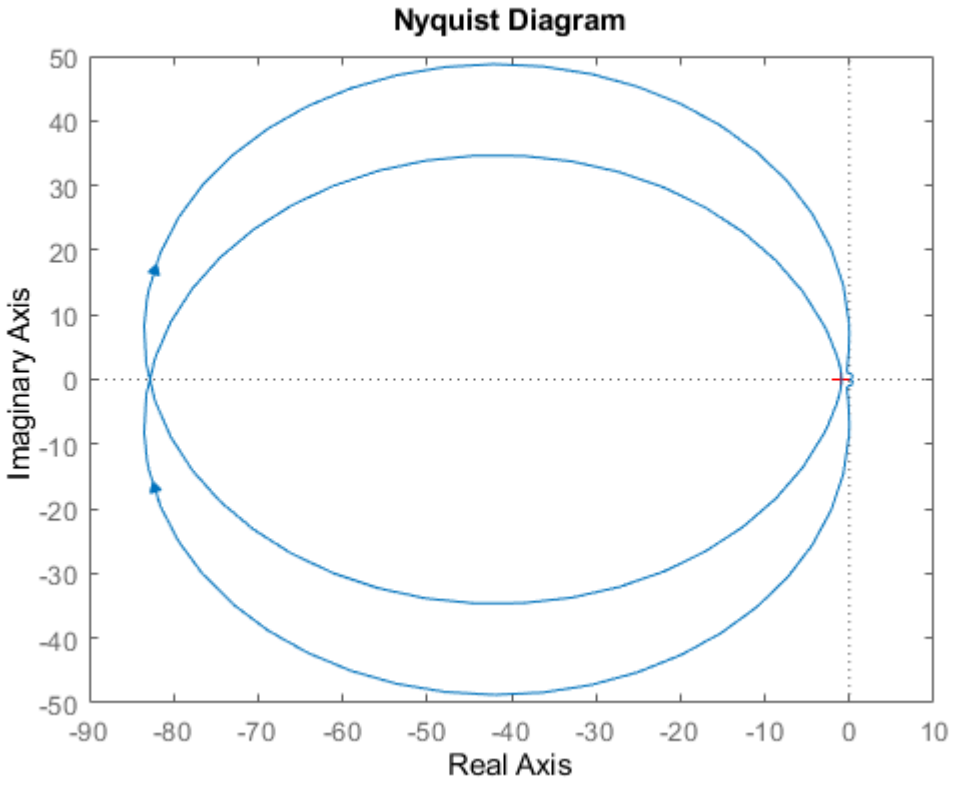

Figure 8 - Nyquist Diagram for Transfer Function of Pitch Angle

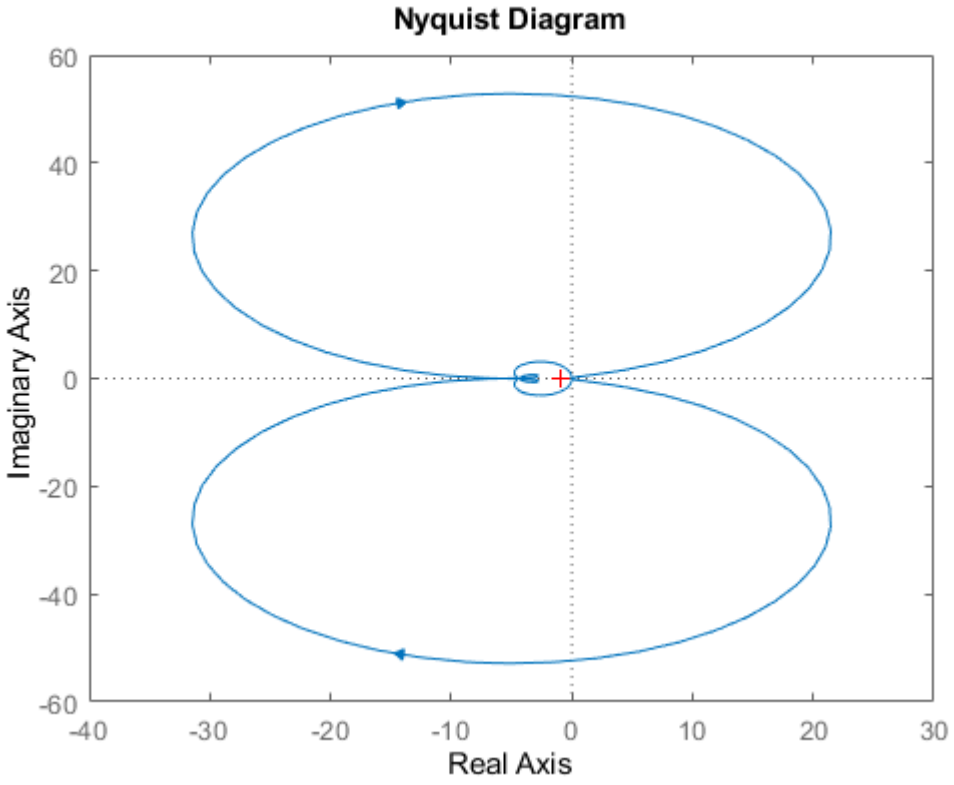

Figure 9 - Nyquist Diagram for Transfer Function of Pitch Rate

D

The measured phase at 0 dB is almost 0.1, so phase margin is 225°. The gain at 180° is -5 dB, so the gain margin is 5 dB. Since phase margin is positive, long period system is stable. The measured gain is 8.95 dB when phase is 180°, so the gain margin is -8.95 dB. 0 dB gain does not exist in short period system. Thus, short period system is stable.

$$G_s = \frac{-2.114s - 0.2262}{s^2 + 0.0256s + 0.402}$$

Is continuous-time transfer function of long-period motion.

$$G_f = \frac{2.114s - 15.02}{s^2 + 6.491s + 42.09}$$

Is continuous-time transfer function of short-period motion.

Natural frequency and damping ratio of the long-period motion are:

Pole	Damping	Frequency (rad/seconds)	Time Constant(seconds)
$-1.28x10^{-2} + 6.34x10^{-1}i$	$2.02x10^{-2}$	$6.34x10^{-1}$	78.1
$-1.28x - +6.34x10^{-1}i$	$2.02x10^{-2}$	$6.34x10^{-1}$	78.1

Natural frequency and damping ratio of the short-period motion are:

Pole	Damping	Frequency (rad/seconds)	Time Constant(seconds)
$-3.25 + 5.62i$	0.5	6.49	0.308
$-3.25 - 5.62i$	0.5	6.49	0.308

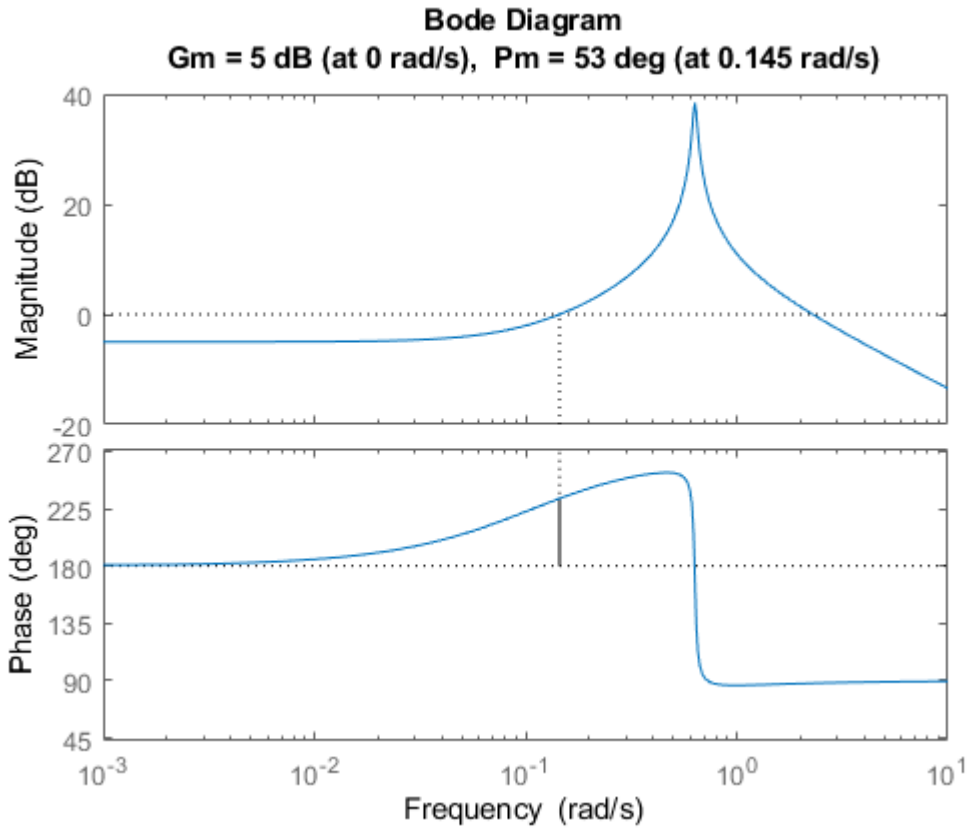

Figure 10 - Bode Diagram for Long Period

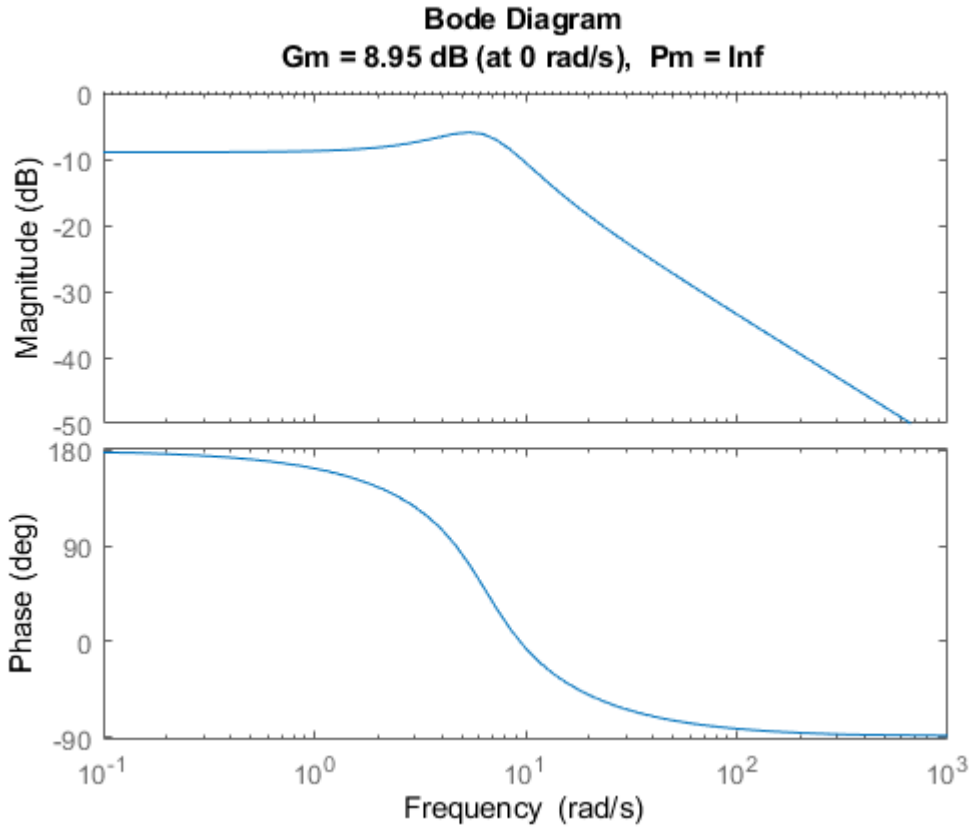

Figure 11 - Bode Diagram for Short Period

E

K values are found from Simulink model which is tuned. The change in pitch angle causes a temporary instability on closed loop function. However, PID controller tries to stabilise it again. Change in pitch angle is caused by pitch rate. As it can be seen in the figure 16, pitch rate is behaving as disturbance to the pitch angle. In figure 17, there is a pole-zero map. According to this figure and figure 4 which is uncontrolled plant pole-z9ero map, PID controller creates different poles and zeros to make the system more stable.

$$C_{pid} = \frac{0.823\,s^2 + 8.84\,s + 16.89}{S}$$

Is continuous*time transfer function of the designed PID controller under the given circumstances.

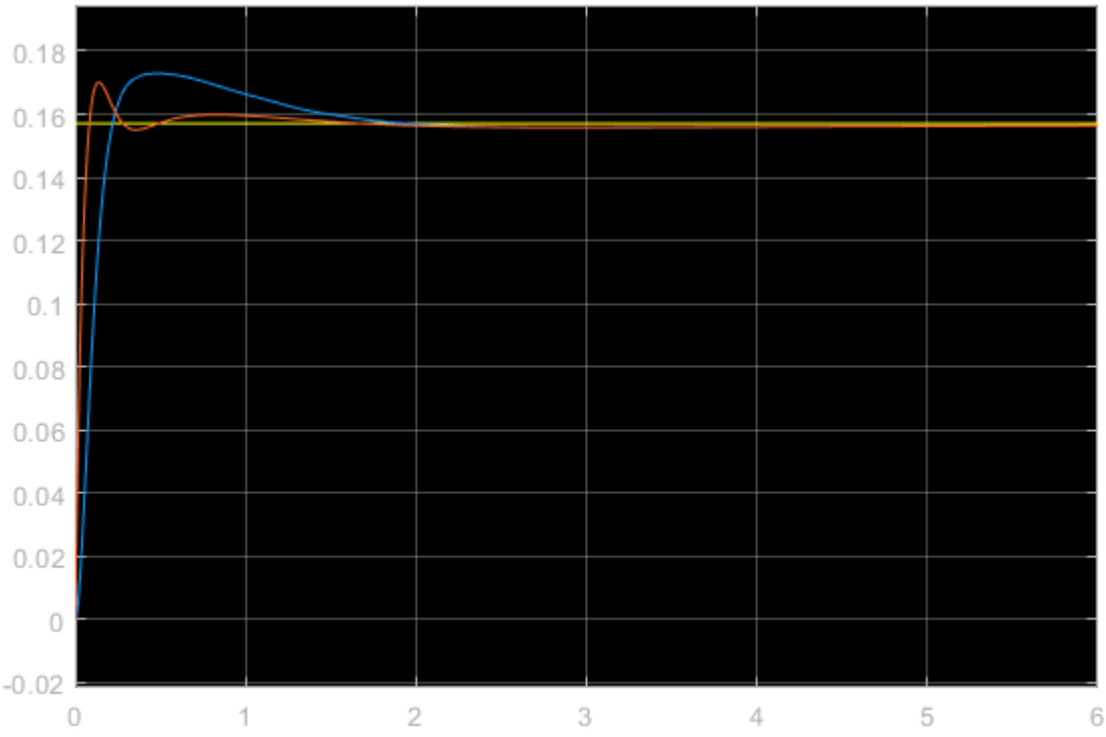

Figure 12 - PID Controller Step Response

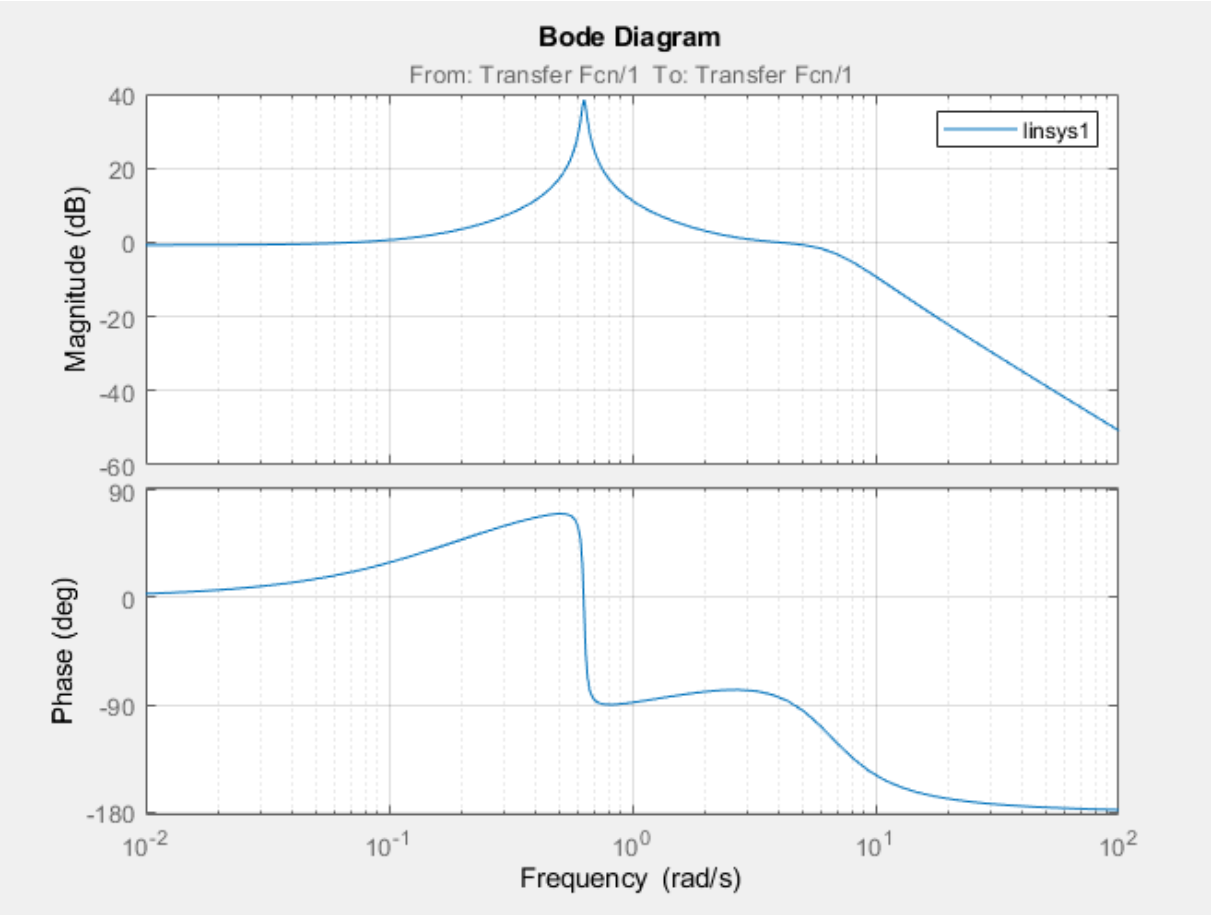

Figure 13 - Bode Diagram for CL

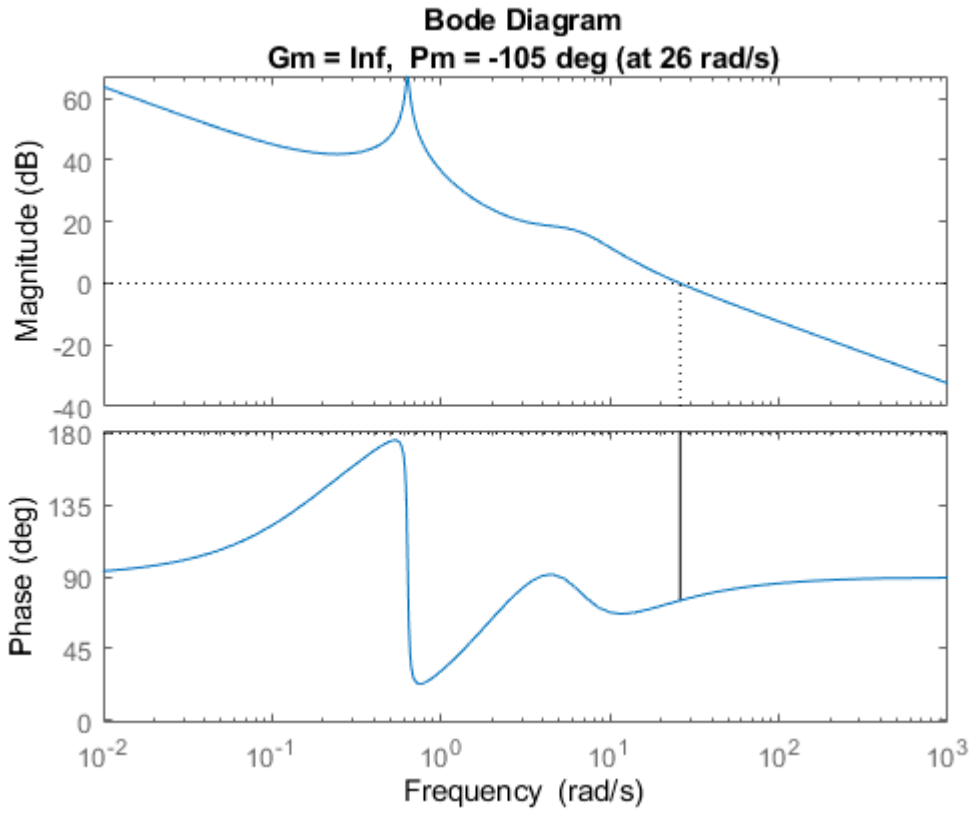

Figure 14 - Bode Diagram for OL

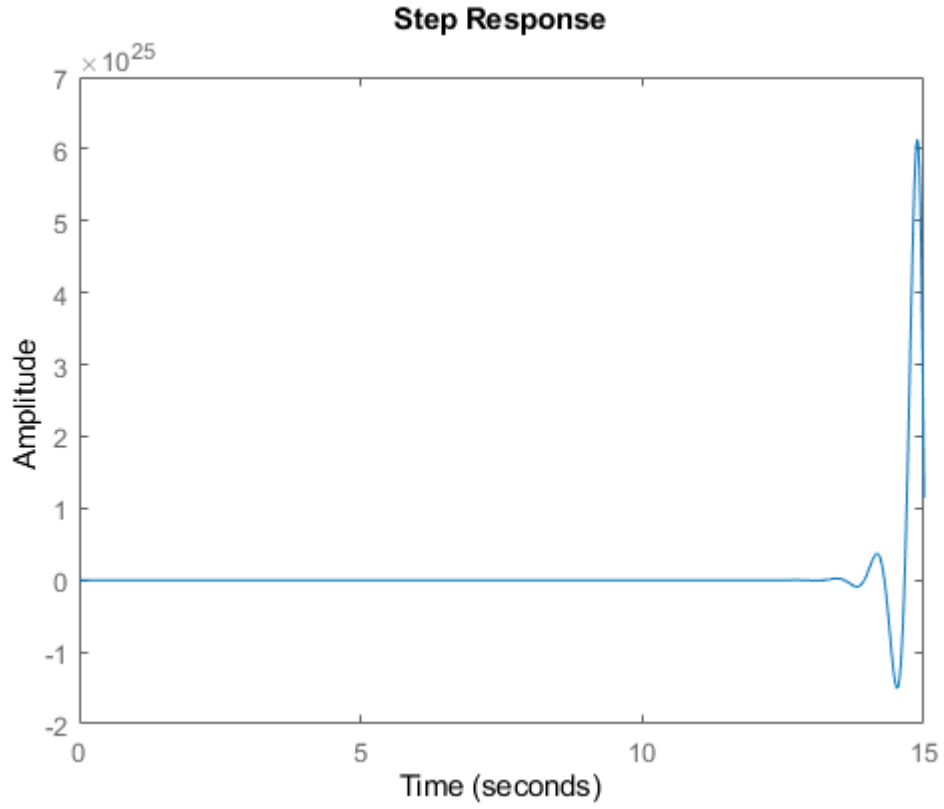

Figure 15 - Step Response for Pitch Angle

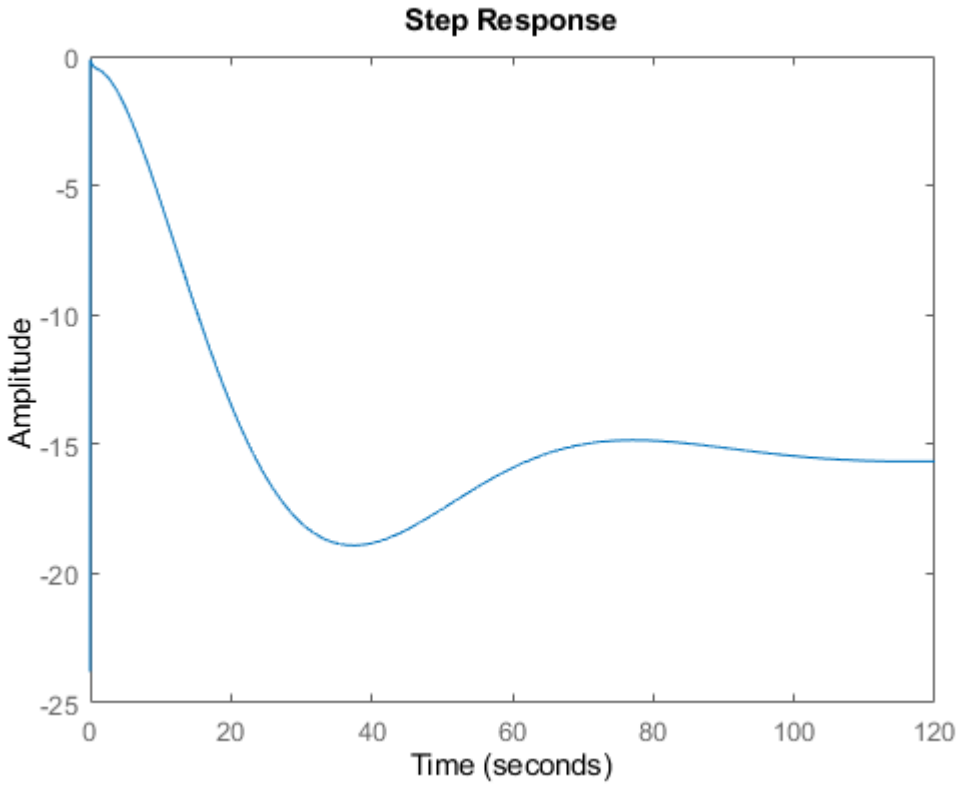

Figure 16 - Step Response for Pitch Rate

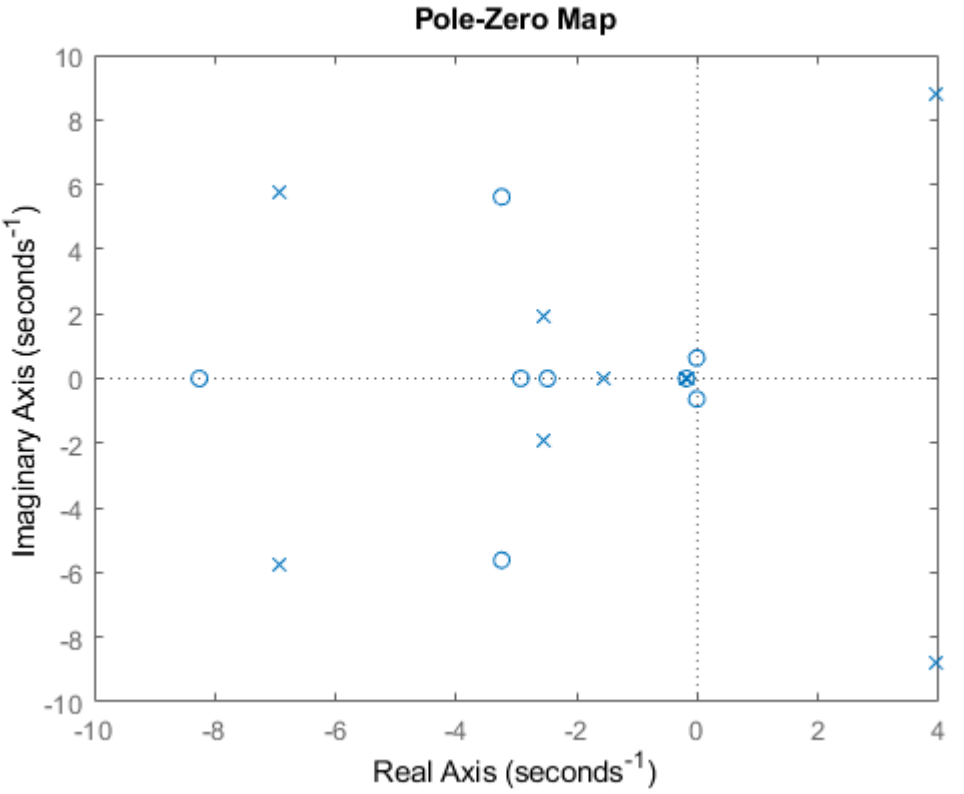

Figure 17 - Pole-Zero Map for CL

F

The expectation is to increase the stability and similarity to the original system as the delay condition decreases. However, results show that similarity to the original system is not a very realistic expectation. Additionally, as the delay condition increases, the stability of the system also increases.

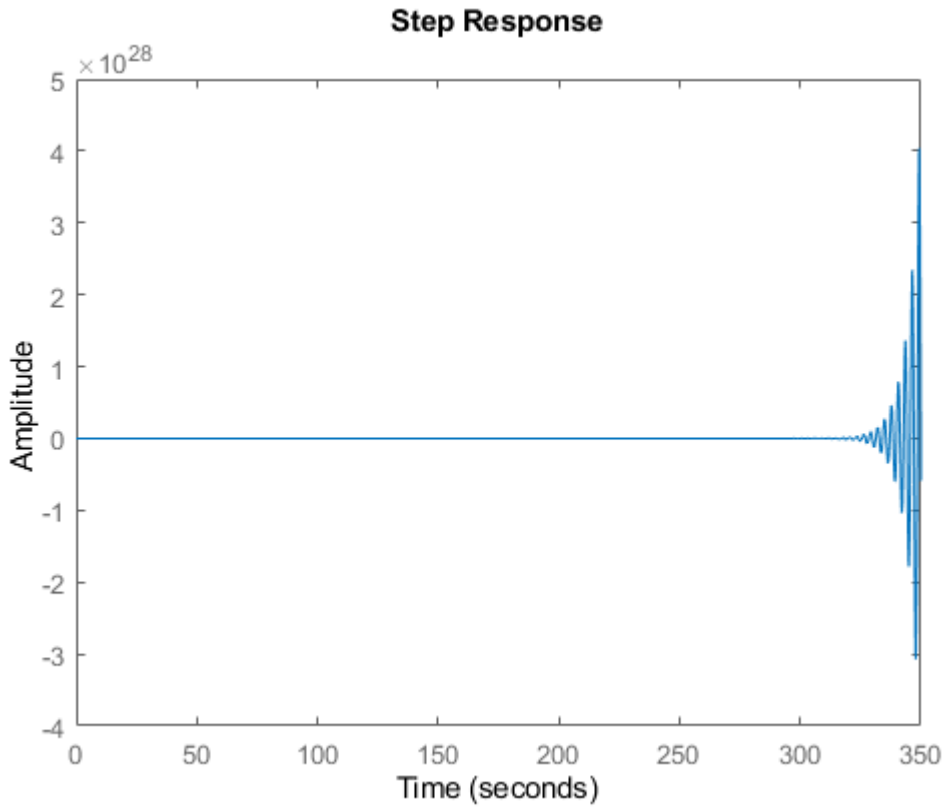

Figure 18 - Step Response for 0.05 second Delay

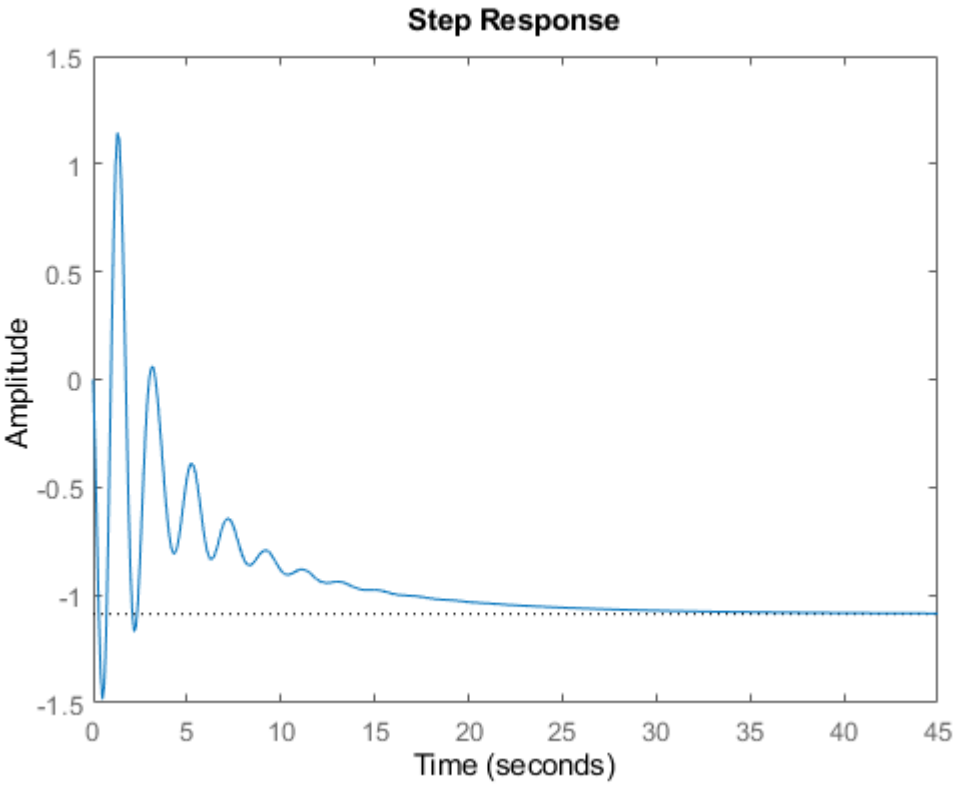

Figure 19 - Step Response for 0.1 second Delay

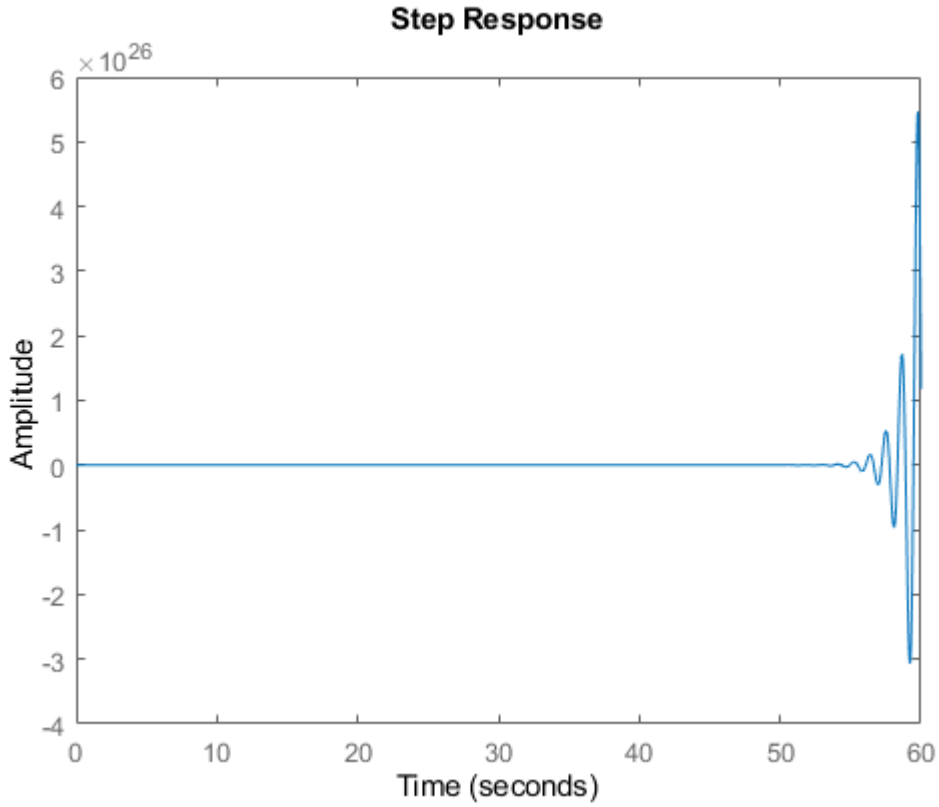

Figure 20 - Step Response for 0.2 second Delay

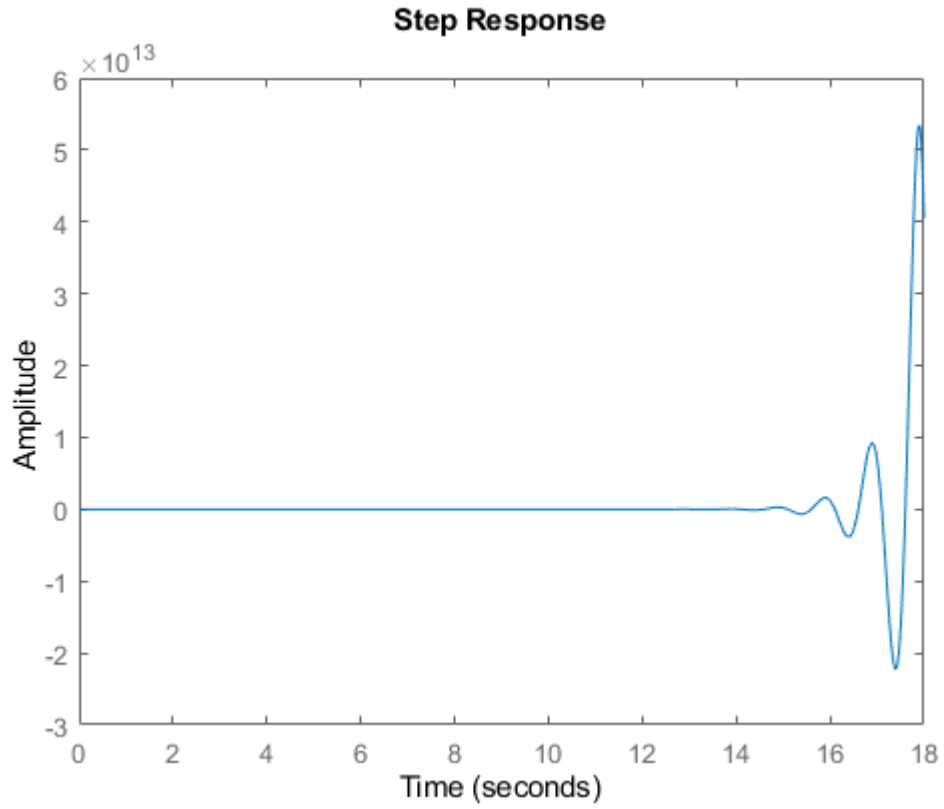

Figure 21 - Step Response for 0.3 second Delay

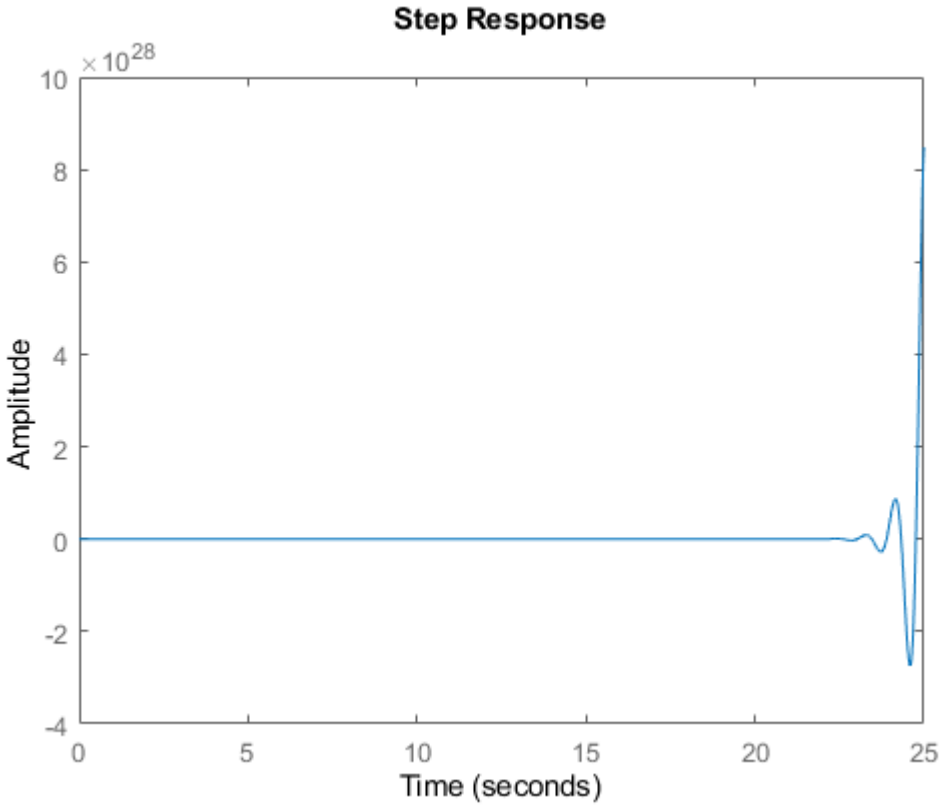

Figure 22 - Step Response for 0.5 second Delay

G

LQR controller gives more stable step response than PID controller. Nevertheless, it will be seen that the difference is not huge when figure 24 and figure 13 are compared. Systems which have either PID controller or LQR controller have almost the same step response. This shows the system has a quite good plant to show behaviours of elevator deflections.

Before designing LQR state controller for the pitch angle control problem, controllability and observability of the system has been checked and concluded that system is fully observable and controllable. Optimal gain matrix of LQR state controller is:

$$K = \begin{matrix} -0.0094 & 0.0476 & -0.5488 & -7.0708 \end{matrix}$$

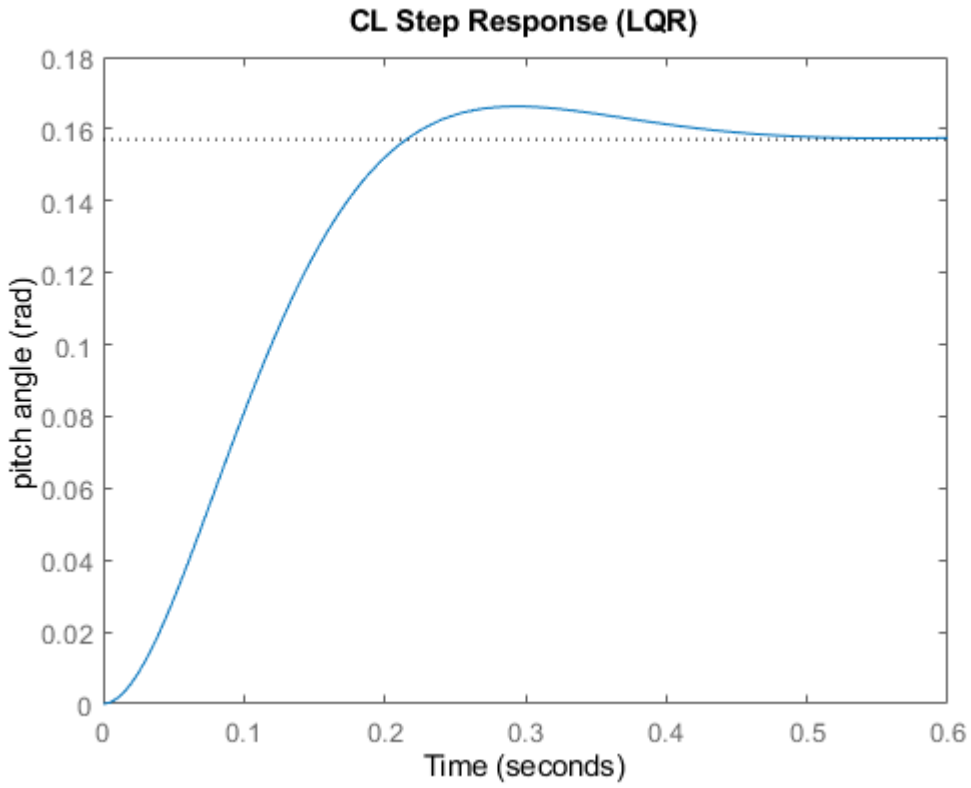

Figure 23 - Step Response for LQR